



LAWRENCE
LIVERMORE
NATIONAL
LABORATORY

The paradox of the tight spiral pass in American football: a simple resolution

R. H. Price, W. C. Moss, T. J. Gay

May 5, 2020

American Journal of Physics

Disclaimer

This document was prepared as an account of work sponsored by an agency of the United States government. Neither the United States government nor Lawrence Livermore National Security, LLC, nor any of their employees makes any warranty, expressed or implied, or assumes any legal liability or responsibility for the accuracy, completeness, or usefulness of any information, apparatus, product, or process disclosed, or represents that its use would not infringe privately owned rights. Reference herein to any specific commercial product, process, or service by trade name, trademark, manufacturer, or otherwise does not necessarily constitute or imply its endorsement, recommendation, or favoring by the United States government or Lawrence Livermore National Security, LLC. The views and opinions of authors expressed herein do not necessarily state or reflect those of the United States government or Lawrence Livermore National Security, LLC, and shall not be used for advertising or product endorsement purposes.

The paradox of the tight spiral pass in American football: a simple resolution

Richard H. Price*

Department of Physics, MIT, 77 Massachusetts Ave., Cambridge, MA 02139

William C. Moss

Lawrence Livermore National Laboratory, Livermore, CA 94550

T. J. Gay

Jorgensen Hall, University of Nebraska, Lincoln, NE 68588-0299

An American football is a rotationally symmetric object which, when well thrown, spins rapidly around its symmetry axis. In the absence of aerodynamic effects, the football would be a torque-free gyroscope and the symmetry/spin axis would remain pointing in a fixed direction in space as the football moved on its parabolic path. When a pass is well thrown through the atmosphere, however, the symmetry axis remains – at least approximately – tangent to the path of motion. The rotation of the symmetry axis must be due to aerodynamic torque, yet that torque, at first glance, would seem to have precisely the opposite effect. Here we explain the action of aerodynamics on the ball's orientation at second glance.

I. INTRODUCTION

A “well-thrown” tight spiral pass in American football exhibits the remarkable property that the long axis of symmetry of the ball appears to maintain tangency with its line of trajectory, i.e., the velocity vector of its center of mass (CM; Fig.1). “Well thrown,” in this context means that the ball has a large angular velocity about its long axis, typically about 600 revolutions per minute¹, and has very little of the “wobble” associated with torque-free precession. Video examples of such a pass can be seen in Ref. 2. In these cases there would appear to be something akin to a negative feedback mechanism that causes the close and continuing alignment of the ball’s long axis with its velocity vector.

If the ball were thrown with the same initial conditions in the absence of air, its long axis would be fixed in space due to the conservation of angular momentum. Thus it is clear that the forces the air exerts on the ball play a crucial role in its attitude. The simplest attempts to explain the tangency of the ball’s axis and its velocity, however, are not satisfactory. The dynamics of rapidly spinning tops don’t provide obvious analogs, nor does a weathervane analogy, with the on-rushing air serving to point it into the “wind.” The simplest version of this explanation fails since the football lacks the front-back asymmetry of a weathervane.

Upon careful consideration of the effect of the air acting on the ball, a more serious question arises, as illustrated in Fig.2. The attitude and flight of the ball can be fully characterized by three vectors: its CM velocity v , the unit vector aligned with its long axis \hat{s} , and its angular momentum L ; for definiteness, we choose \hat{s} to be in the direction such that the angle between it and L is acute. For a “perfect” spiral pass, v , \hat{s} , and L are initially co-linear. (If L and \hat{s} are not aligned, the ball will wobble with \hat{s} executing approximately torque-free precession about L .) As gravity causes v to tilt downward after the ball is launched, the aerodynamic force F begins to produce a so-called “pitch torque” (or “moment”) that points into the diagram along $+\hat{y}$. Indeed, one envisions that such a torque into the page will always exist in that the line of the trajectory will continue to fall away from the ball’s axis over the course of the arc of the pass.

The following paradoxical situation now becomes evident. Assuming a simple planar parabolic trajectory as shown in Fig.1, the ball’s initial angular momentum will have the form $L_i = a\hat{z} + b\hat{x}$, where a and b are positive. The ball’s final angular momentum is $L_f \approx a\hat{z} - b\hat{x}$ when it is caught. The angular momentum change $L_f - L_i$ is thus $-2b\hat{x}$, while the aerodynamic torque discussed in the previous paragraph, integrated over the ball’s flight time would, paradoxically, appear to lie along \hat{y} .

This puzzle regarding the ball’s orientation and the mechanism that keeps the ball’s symmetry axis more-or-less aligned with the velocity vector along its trajectory are what we consider in this paper. The general problem of the flight of an American football

was, to our knowledge, first considered by Brancazio^{3,4}, who analyzed the wobble of the ball and suggested that the trajectory alignment of a tight spiral pass could be explained in terms of a rapidly spinning “sleeping” top, i.e., one that maintains its vertical orientation despite the application of perturbative horizontal torques. This analogy seems to us to be inappropriate, given that the ball experiences continuous aerodynamic torque throughout the duration of its flight instead of brief, perturbative torques. Subsequent wind tunnel tests by Rae and Streit⁵ and by Watts and Moore⁶ determined football drag and spin-drag coefficients that have provided useful input data for more recent models of the ball’s flight. The most detailed analyses of tight spiral flight to date have been conducted by Rae¹, Soodak⁷, and by Seo, Kobayashi, and Murakami⁸. Rae’s approach essentially integrates Euler’s equations and, using the wind-tunnel data he and Streit collected, calculates the pitch, yaw, and azimuthal rotation of a pass that are compared to detailed videographic data. Seo, Kobayashi, and Murakami followed Rae’s approach for a kicked rugby ball spiral, using data from their own wind tunnel tests. Soodak used a perturbative analytical approach to solve Euler’s equations and considered the motion for limited launch cases that are consistent with his approximations. Gay⁹ provided a critical overview of the football papers listed above and considered a number of novel aspects of the ball’s flight.

The goal of this paper is to explain clearly and simply the reason why a well-thrown spiral pass maintains approximate tangency with its line of trajectory. In doing so, we resolve the paradox mentioned above. The solution to this problem is also contained in the work of Rae and Soodak, but is somewhat obscured by the detailed mathematics (in the case of Soodak) or the largely computational approach taken (Rae), and by the fact that neither has focused on this phenomenon.

Our paper has the following organization. Section 2 will introduce the dynamical equations and the basic approximations we use. Section 3 introduces the relevant dynamical quantities for a “long bomb” tight spiral pass and presents the results of numerical calculations using the analysis introduced in Sec. 2. Section 4 explains the essence of the mechanism by which the interaction of the aerodynamic torque and angular dynamics keeps the symmetry axis approximately aligned with the velocity vector. In Sec. 5, we consider the effect of throwing a less-than-perfect spiral pass with a bit of wobble to it, illustrating the addition of quasi-torque-free precession to the ball’s flight. Section 6 presents a simple analytical solution that describes the ball’s attitude when some reasonable approximations are made, and that justifies our resolution of the paradox in a more explicitly mathematical way. We conclude and summarize in Sec. 7.

Values throughout the paper are in SI units; a circumflex over a symbol (\hat{x}) indicates a unit vector or a component of a unit vector; an overdot indicates a time derivative; both radian and degree measures of angles are used as indicated.

II. BASIC EQUATIONS AND SIMPLIFYING ASSUMPTIONS

The forces that the air exerts on the moving ball are complicated; the Reynold's numbers associated with the ball's CM motion and its spin indicate that the flow of air over the ball's surface is largely turbulent. Based on the wind tunnel tests of Refs. 5 and 6 however, these forces can be described heuristically and resolved into a single net force acting through the ball's CM, and a force couple that exerts a pure torque about the CM. This couple can further be resolved into a "spin-drag" torque along $\hat{\mathbf{s}}$, and a second torque $\boldsymbol{\tau}$ that acts about the CM in a direction perpendicular to $\hat{\mathbf{s}}$. This latter torque is the result of the "angle of attack" between $\hat{\mathbf{s}}$ and $\hat{\mathbf{v}}$, as indicated in Fig.2. In our analysis, we neglect the spin-drag torque. We also ignore the net drag force on the ball, so that we take the ball's CM position to be determined solely by its kinematic initial conditions and the force of gravity. Thus \mathbf{v} will always be tangent to a parabolic trajectory lying in the xz plane. The only effect of air drag in our calculations is thus to change the ball's attitude, i.e., its pitch and yaw; these angles are all we need to understand the trajectory-following phenomenon and to resolve the paradox.

Following Soodak^{7,10}, we start with

$$\dot{\mathbf{L}} = \boldsymbol{\tau} \quad (1)$$

and

$$\dot{\hat{\mathbf{s}}} = (1/I_t)\mathbf{L} \times \hat{\mathbf{s}}, \quad (2)$$

where I_t is the ball's moment of inertia about any axis perpendicular to its long symmetry axis and through its CM. Equation (1) is the fundamental equation of rotational dynamics. Equation (2) is less well known. A derivation of it is given by Soodak but, in view of the importance of this equation for our analysis, a derivation is given in the Appendix.

Soodak assumes that this torque can be approximated by $\boldsymbol{\tau} = \kappa(\hat{\mathbf{v}} \times \hat{\mathbf{s}}) \propto \sin\theta_{vs}$, where κ is a constant and θ_{vs} is the angle of attack. We note, however, that $\boldsymbol{\tau}$ must vanish as θ_{vs} approaches $\pi/2$. Indeed, Rae and Streit⁵ have shown in their wind tunnel experiments that a better expression for the torque magnitude is $\kappa\sin 2\theta_{vs}$. Since we consider here only small angles of attack associated with a "tight spiral" pass, for the aerodynamic torque we will use the approximation

$$\boldsymbol{\tau} \approx 2\kappa(\hat{\mathbf{v}} \times \hat{\mathbf{s}}) \equiv \tau^*(\hat{\mathbf{v}} \times \hat{\mathbf{s}}), \quad (3)$$

where τ^* remains a heuristic constant that depends primarily on the football's size, shape, and speed through the air. Our analysis then is based on two equations: Equation (2) and

$$\dot{\mathbf{L}} = \tau^*(\hat{\mathbf{v}} \times \hat{\mathbf{s}}). \quad (4)$$

III. TAKING THE EQUATIONS TO THE FIELD

We now consider a typical “long bomb” football pass which best illustrates the trajectory-following phenomenon we wish to explain. We use parameters similar to those considered by Rae (listed in Table 1): a launch angle θ above the horizontal of 30° (the initial direction of \mathbf{v}) and a launch speed v_0 of 27.4 m s^{-1} (61 mph). Because of our neglect of air drag on the ball’s CM motion, the ball’s flight is parabolic with a duration T of 2.80 s and a range R down field of 66.4 m (72.7 yards). The long axis of the ball, its CM-velocity, and its angular momentum are all taken to lie initially in the xz plane (in which \mathbf{v} will remain). We assume that the ball is thrown either perfectly or almost perfectly. In the latter case we will allow for some “wobble,” caused in this analysis by an initial nonzero pitch of the ball above the initial launch angle, so that \mathbf{v} , \mathbf{L} , and $\hat{\mathbf{s}}$ are not initially co-linear.

The motion of the football can be characterized by four rotational rates: (i) the angular speed of the ball about its long axis, ω_{spin} ; (ii) the angular rate, ω_{wob} , at which the ball wobbles, i.e., at which $\hat{\mathbf{s}}$ executes approximately torque-free precession about \mathbf{L} ; (iii) the angular rate ω_{gyr} at which the ball precesses “gyroscopically” due to the torque caused by its angle of attack in the air stream; and (iv) the rate at which $\hat{\mathbf{v}}$ rotates in the xz plane due to gravity, ω_{traj} . The characteristic rates ω_{wob} and ω_{gyr} are given by⁷

$$\omega_{wob} = L/I_t \approx \omega_{spin} I_l/I_t \quad (5)$$

and

$$\omega_{gyr} = \tau^*/L, \quad (6)$$

where I_l is the moment of inertia of the ball about its long axis. Using quantities that are available in the literature, we can determine the rotation rates that are relevant for the problem. For the “long bomb”, these are listed in Table I. We note that for a well-thrown pass with just a bit of wobble, ω_{gyr} will generally be $\sim 2.5 \text{ rad/s}$. This precessional rate is approximately independent of the angle of attack, in the same way that the precessional rate of a rapidly spinning top is independent of the angle its axis makes with the vertical.¹¹

We begin by integrating Eq.(2) and Eq.(4) numerically, using the values of Table I and initial conditions corresponding to a perfect spiral pass, i.e., one in which \mathbf{v} , $\hat{\mathbf{s}}$, and \mathbf{L} are initially co-linear. The resulting solution shows that \mathbf{L} and $\hat{\mathbf{s}}$ track each other very closely over the course of the flight. Indeed, we find this to be the case for all of the initial conditions we consider in this paper. Thus, we can use the approximation

$$\mathbf{L} \approx L\hat{\mathbf{s}}. \quad (7)$$

To obtain a clearer picture of the extent to which the symmetry axis $\hat{\mathbf{s}}$ deviates from the line of tangency $\hat{\mathbf{v}}$, we consider the “deviation vector,” $\mathbf{S} \equiv S_X\hat{\mathbf{X}} + S_Y\hat{\mathbf{Y}}$, which is

the projection of $\hat{\mathbf{s}}$ on a plane perpendicular $\hat{\mathbf{v}}$, To this end, we specify the orthonormal coordinate system $(\hat{\mathbf{X}}, \hat{\mathbf{Y}}, \hat{\mathbf{v}})$, defined by the vectors $(\hat{\mathbf{y}} \times \hat{\mathbf{v}}, \hat{\mathbf{y}}, \hat{\mathbf{v}})$. The components of \mathbf{S} are thus

$$S_Y = \hat{s}_y ; S_X = \hat{v}_z \hat{s}_x - \hat{v}_x \hat{s}_z , \quad (8)$$

where, e.g., \hat{v}_z is the component of $\hat{\mathbf{v}}$ along z . For small misalignment of the symmetry axis and the velocity vector, \mathbf{S} measures the approximate angle of the misalignment (in radians); for perfect alignment $\mathbf{S}=0$.

Figures 3 and 4 show the computed time and parametric development of S_X and S_Y . The results are comparable to those shown in Rae's¹ Fig 9. In making the comparison between our results and those of Rae, it should be noted that our S_X corresponds to Rae's aerodynamic "pitch" $\tilde{\alpha}$, but our S_Y is the negative of Rae's aerodynamic "yaw", $\tilde{\beta}$, which he calls "slideslip"¹. Thus the fact that the path of the deviation is clockwise in our Fig.4 is consistent with the counterclockwise path in Rae's Fig.9. Figure 4 can be regarded as showing the pitch and yaw of the ball as viewed by the quarterback who throws the ball, as opposed to the receiver who is looking over his shoulder to catch it. The quantitative differences between our results and those of Rae can be ascribed to the details that Rae includes but we do not, such as wind drag on the CM motion of the ball. This reduces its speed, and results in a non-planar, non-parabolic line of trajectory that veers to the right, as seen by the (right-handed!) quarterback.^{1,12} However, the qualitative agreement between our results and those of Rae with respect to the ball's attitude over its flight time justifies our simplifications.

Given the perfect launch of the ball, its wobble is barely noticeable, appearing as a small-amplitude high-frequency "scalloping" of the smooth curves shown in Figs. 3 and 4. In Fig. 4, The tip of the deviation vector, \mathbf{S} , rotates with an angular frequency of about 2.52 rad/s - in excellent agreement with ω_{gyr} - about a point at roughly $(S_X, S_Y) = (0, 0.15)$. This point corresponds to zero pitch and a yaw of $\sim 9^\circ$.

IV. RESOLVING THE PARADOX

The heart of the resolution of our football paradox lies in the response of the football to the aerodynamic torque caused by the non-zero angle of attack that develops after its launch, assumed for this discussion to be that of a perfect spiral pass. To illustrate this idea, we neglect gravity and assume that the football is moving in a straight line in the $+z$ direction. If $\hat{\mathbf{s}}$ and \mathbf{L} are both in the z -direction, nothing interesting happens, so we now tilt the front of the football slightly upward, i.e., in the positive x direction. (This is the equivalent of the trajectory turning downward under the action of gravity in the actual pass.) The airflow then imposes a torque in the $+\hat{\mathbf{y}}$ direction as shown in Fig.5a. Since \mathbf{L} is essentially in the same direction as $\hat{\mathbf{s}}$, the torque causes $\hat{\mathbf{s}}$ to develop a

component along $+\hat{y}$, i.e., gyroscopic precession results in the ball yawing right. In this position, as shown in Fig.5b, the aerodynamic torque develops a component in the $-x$ direction, giving rise to a component of precession about \hat{y} , so the ball starts to tip downward. (In the case of an actual pass immediately after launch, this torque along $-x$ results in a slowing of the growth of the S_x component (see Fig.4)). Put simply, the gyroscopic precession resulting from the pitch- and yaw-induced aerodynamic torque, coupled with the co-linearity of L and \hat{s} , causes $dS_y/dt \propto S_x$ (Fig.5a), and $dS_x/dt \propto -S_y$ (Fig.5b), which means that the tip of S moves in a circle with an angular frequency ω_{gyr} .

With this simple case in mind, we now consider what happens in a real pass after the ball has been launched. Again we suppose that \hat{v} , L , and \hat{s} are initially aligned. After the launch, however, \hat{v} begins to slowly rotate downward under the action of gravity. By “slowly”, we mean that the rate at which the velocity direction rotates is significantly smaller than the other relevant rotation rate, ω_{gyr} . (In our example, the rate of \hat{v} 's rotation is about 0.37 rad/s.) A result of the change in \hat{v} is that it loses alignment with \hat{s} , and the subsequent angular dynamics are dominated by the aerodynamic torque associated with the non-zero angle of attack. Consequently, the tip of S (Eq.(8)) executes a quasi-circular motion, as described in the previous paragraph.

An obvious question is why, during this quasi-circular motion, the vertical torque on the football is not “averaged out”? We can find the answer by taking the time average of the x component of Eq.(4):

$$\langle \dot{L}_x \rangle = -\tau^* \langle \hat{v}_z \hat{s}_y \rangle. \quad (12)$$

The football points “forward” throughout the pass (Fig.1), so \hat{v}_z is always positive. The average downward ($-x$) torque can therefore be ascribed to the fact that $S_y = \hat{s}_y$ is biased to positive values, as is evident from Figs.4 and 5a. This is due, in turn, to the fact that v is constantly turning downward along the arc of the pass, so that there is always a tendency for positive pitch to develop, with its subsequent driving of the ball's gyroscopic precession to the right.

This is the essential resolution of the football paradox: The angular dynamics of S is dominated by the aerodynamic torque due to the non-zero angle of attack, and this angular dynamics requires that S move in a circle of a small radius. This radius is the measure of misalignment of \hat{s} and \hat{v} . That it remains small means that the alignment remains good.

Figure 4 nicely illustrates the above discussion. We see that the approximately closed path of the tip of S in the XY plane does not grow in time. While v rotates by $\pi/3$ from 30° to -30° , S is confined to motion with a radial extent of only 13% of that rotation. When the deviation develops a $+x$ component due to gravity, there is a torque in the $+y$

direction and the deviation is driven to more positive y . As the $+y$ component increases, however, S is driven below the velocity tangent, leading to an almost complete elimination of the ball's yaw. In this way, the deviation is driven in the clockwise pattern shown. A crucial feature of this pattern is that the deviation is not symmetric about $S_Y = 0$; the more S deviates in the $+y$ direction the stronger the aerodynamic torque is in the $-x$ direction. Because the deviation spends all of its time in territory with positive S_Y , the torque is strongly in the $-x$ direction essentially all of the time. This is why the ball's axis can so closely track the ever down-tipping velocity vector.

It must also be pointed out that our results (as well as those of Rae's) do not support our initial observation that "...the long axis of symmetry of the ball appears to maintain tangency with the line of its trajectory", or that "...there would appear to be something akin to a negative feedback mechanism that causes the close and continuing alignment between the ball's axis and its velocity." These statements are now seen to be qualitatively, but not quantitatively correct. The ball's attitude throughout the course of the flight certainly remains strongly correlated with its axis, but this correlation is not the result of negative feedback. It is instead due to the ball's tendency to gyroscopically precess smoothly about the axis of the aerodynamic drag force. Our analysis shows that even for a perfectly-thrown tight spiral pass, the ball's axis just before it is caught will have a small yaw to the right (as seen by our right-handed quarterback), and a small positive or negative pitch as well. The yaw and pitch angles, however, remain small even for a "long bomb" as we have shown, and the fan in the stands, or the television watcher viewing an instant replay, may be excused for being impressed by the illusion of a perfectly aligned ball.

V. THE LESS-THAN-TIGHT SPIRAL PASS

To illustrate the role of quasi-torque-free precession on the ball's flight, we now consider an example of a pass described by the parameters in Table I, but that, rather than starting perfectly, has an initial 10° upward pitch with no yaw, i.e. $S_X = 0.175$ and $S_Y = 0$. We have chosen these initial conditions to allow comparison with the numerical results of Rae¹. The results for the computed time development of pitch and yaw are shown in Figs. 6 and 7. The ball executes about 1.17 low-frequency oscillations during the 2.8 s pass, again with an angular frequency in good agreement with ω_{gyr} . The approximately 14.7 small nutation-like oscillations during the flight have a period of 0.19 s, in acceptably good agreement with the 0.17 s period for $\omega_{wob} = 38.0$ rad/s. Interestingly, because of the initial pitch, the gyroscopic precessional radius now increases from the perfect-pass case of 0.15 to ~ 0.22 . Thus the average deviation angle between \hat{s} and \hat{v} increases significantly. Importantly, however, the center of precession remains the same at a zero-pitch yaw of 9° ; the ball still tracks the line of trajectory closely.

The path of \mathbf{S} in Fig.7 can be compared directly to the result shown in Fig.5 of Rae's paper¹. That figure shows roughly 1.5 slow oscillations during the 3 s flight, and roughly 20 high-frequency cycles. We note that our results agree with Rae's in showing that the direction of the symmetry axis is vertically symmetric, i.e. symmetric about $S_x = 0$, just as Rae's results are symmetric about $\tilde{\alpha} = 0$. However, in our calculation, the yaw angle does veer into $-y$ territory for a brief period between 1.7s and 2.2s into its flight.

There is a significant difference between the pattern of high-frequency loops in Rae's Fig.5, and the pattern of cusps in our Fig.7. The difference can be ascribed to shifts in phase of the pitch and yaw. It is interesting that the looping is almost absent early in Rae's Fig.5, suggesting that it requires details such as the effect of air drag on the shape of the trajectory not included in our model; that effect might be significant only late in the trajectory.

VI. A SIMPLIFIED ANALYTICAL MODEL

In analytically exploring the model of Eqs.(2) and (4), the actual path of a football under gravity is a complicating factor, since the rate at which $\hat{\mathbf{v}}$ rotates is variable. We will, therefore, sacrifice some reality for simplicity by using a "circular" model for the change of $\hat{\mathbf{v}}$:

$$\hat{\mathbf{v}}_z = \cos(\Omega t) ; \hat{\mathbf{v}}_x = -\sin(\Omega t), \quad (13)$$

where Ω is the angular velocity of the rotation of $\hat{\mathbf{v}}$ in the xz plane, and is taken to be constant. To maintain some connection to the more realistic model of Section 2, in which the football turns by $\pi/3$ radians in 2.8 s, we take the (now constant) value of $\Omega = 0.374$ rad/s. (For the "long bomb" parabolic trajectory, the actual rate of rotation of $\hat{\mathbf{v}}$ deviates by 17% below and 10% above this average.) All other relevant parameters are taken from Table I.

We now make two more simplifying assumptions, both of which are justified by our numerical results presented above. First, we assume $\hat{\mathbf{s}}$ and \mathbf{L} are always well-aligned (i.e., Eq.(7)) and that, more precisely, that they are much better aligned than are $\hat{\mathbf{s}}$ and $\hat{\mathbf{v}}$. In fact, for the perfectly-thrown "long bomb" of Figs.3 and 4, $(\mathbf{L} \cdot \hat{\mathbf{s}})/L$ varies by less than 2×10^{-4} , while $\hat{\mathbf{v}} \cdot \hat{\mathbf{s}}$ varies by 4×10^{-2} . Secondly, we take the magnitude of \mathbf{L} to be constant; our full numerical solution indicates that it varies by only about 2 parts in 10^4 .

Our analysis begins at $t = 0$ when the ball is at the zenith of its trajectory, with $\hat{\mathbf{s}}$ and \mathbf{L} exactly aligned with $\hat{\mathbf{v}}$. With our assumptions, Eq.(4) becomes

$$\dot{\hat{\mathbf{s}}} = \omega_{gyr}(\hat{\mathbf{v}} \times \hat{\mathbf{s}}). \quad (14)$$

When combined with Eqs.(8) and (13) this yields

$$\dot{S}_X = -\omega_{gyr}S_Y - \hat{s}_z\dot{\hat{v}}_x + \hat{s}_x\dot{\hat{v}}_z = -\omega_{gyr}S_Y + \Omega(\hat{s}_z\hat{v}_z + \hat{s}_x\hat{v}_x) = -\omega_{gyr}S_Y + \Omega \quad (15a)$$

and
$$\dot{S}_Y = \omega_{gyr}S_X. \quad (15b)$$

Equations (15) show that S_X and $S_Y - \Omega/\omega_{gyr}$ should exhibit simple harmonic oscillations with angular frequency ω_{gyr} . For perfect initial alignment, i.e., for $S_X = S_Y = 0$ at $t = 0$, the equations predict

$$S_X = (\Omega/\omega_{gyr})\sin \omega_{gyr}t \quad (16a)$$

and

$$S_Y = (\Omega/\omega_{gyr})[1 - \cos \omega_{gyr}t]. \quad (16b)$$

Figure 8 shows the analytical results for S_X and S_Y of Eqs.(16). The numerical results are the output of computation of Eqs.(2) and (4) (i.e., Figs.3 and 4) with no *a priori* assumptions about the variation of L or the alignment of $\hat{\mathbf{s}}$, L and \mathbf{v} after $t = 0$. The two sets of results show rather good agreement, giving us confidence that the approximations used to obtain Eqs.(16) do not undermine their simple analytical demonstration of the trajectory-following phenomenon. Indeed, these equations give us the clearest resolution of the paradox stated at the beginning of the paper.

The rotational angular velocity, Ω , of $\hat{\mathbf{v}}$ in Eq.(15a), which depends strongly on the gravitational acceleration, is the driver of the process that keeps the ball's major symmetry axis aligned with its trajectory. If Ω is removed from Eq. (15a), Eqs.(16) describe circular motion with an amplitude that is undetermined by the parameters of the problem. But with the second term in the RHS of Eq.(15a), the amplitudes of the components of S are determined by Ω/ω_{gyr} , which is significantly less than unity. It is thus the relatively slow rotation of the ball's velocity vector that locks the deviation vector S into a small circle, and the symmetry axis into alignment. We note also that Eq.(16b) shows explicitly that the ball's symmetry axis is biased toward positive y , demonstrating analytically the arguments accompanying Eq.(12) that explain why the nose of the football descends.

The agreement between the numerical and approximate analytical solutions shown in Fig. 8 are noticeably improved by a more involved analytical treatment in which no assumptions are made about misalignments or the variation of L , except that all are small. This analysis will be presented in a future publication¹³.

VII. CONCLUSION

We have analyzed the paradox of how an American football, thrown in a tight spiral pass, maintains the close alignment of its long axis with its trajectory. We have

shown that the paradox is simply resolved by focusing on the gyroscopic precession driven by the torque that results from the ball's non-zero angle of attack, and by the interaction of that torque with the ball's angular momentum. Some previous analyses, in our opinion, have treated the high-frequency torque-free precession on an equal footing with the relatively slow precession driven by the aerodynamic torque. The high-frequency precession, however, is not central to the resolution of the pass paradox, and clearly distinguishing the two types of precession has been the key to a clear explanation.

Acknowledgments

This work was supported in part by NSF Grant PHY1806771 (TJG), and under the auspices of the U.S. Department of Energy by Lawrence Livermore National Laboratory under Contract DE-AC52-07NA27344 (WCM). The authors would like to thank the two referees of this paper, who provided detailed, helpful comments on an earlier version of the manuscript.

APPENDIX: DERIVATION OF EQUATION 2

Let \hat{t} be a unit vector perpendicular to \hat{s} such that the instantaneous angular velocity $\boldsymbol{\omega}$ can be written as

$$\boldsymbol{\omega} = \omega_s \hat{s} + \omega_t \hat{t}, \quad (\text{A1})$$

and, due to the symmetry of the moment of inertia tensor, the total angular momentum can be written as

$$\mathbf{L} = I_s \omega_s \hat{s} + I_t \omega_t \hat{t}. \quad (\text{A2})$$

For any vector \mathbf{a} fixed in the rotating body, its time derivative due to the rotation is given by $\dot{\mathbf{a}} = \boldsymbol{\omega} \times \mathbf{a}$, and hence, with Eq.(A2), we have

$$\dot{\hat{s}} = \boldsymbol{\omega} \times \hat{s} = \omega_t \hat{t} \times \hat{s} = \frac{1}{I_t} \mathbf{L} \times \hat{s}, \quad (\text{A3})$$

which completes the derivation.

REFERENCES

*Electronic address: rhprice@mit.edu

- 1) William J. Rae, "Flight dynamics of an American football in a forward pass," *Sports Engineering* **6** 149-163 (2003).
- 2) <https://www.youtube.com/watch?v=AciLf7dAh9s>
- 3) Peter J. Brancazio, "Rigid-body dynamics of a football," *Am. J. Phys.* **55**(5) 415-420 (1987).
- 4) Peter J. Brancazio, "The physics of kicking a football," *The Physics Teacher*, **23**, 403-407 (1985); <https://doi.org/10.1119/1.2341866>
- 5) W. J. Rae and R. J. Streit, "Wind-tunnel measurements of the aerodynamic loads on an American football," *Sports Engineering* **5**, 165-172 (2002).
- 6) Robert G. Watts and Gary Moore, "The drag force on an American football," *Am. J. Phys.* **71**, 791-793 (2003).
- 7) Harry Soodak, "A geometric theory of rapidly spinning tops, tippe tops, and footballs," *Am. J. Phys.* **70**(8) 815-828 (2002).
- 8) K. Seo, O. Kobayashi, and M. Murakami, "Flight dynamics of the screw kick in rugby," *Sports Engineering* **9** 49-58 (2006).
- 9) T. J. Gay, *The Physics of Football* (Harper-Collins, New York, 2005), Chap. 6.
- 10) F. Scheck, *Mechanics – From Newton's Laws to Deterministic Chaos*, 2nd edition (Springer-Verlag, Berlin, 1994).
- 11) Daniel Kleppner and Robert Kolenkow, *An Introduction to Mechanics*, 2nd ed. (Cambridge, 2014), p.302.
- 12) Bart Starr with Mark Cox, *Quarterbacking* (Prentice-Hall, Englewood Cliffs, New Jersey, 1967), pps. 168-169.
- 13) Richard H. Price, to be published.

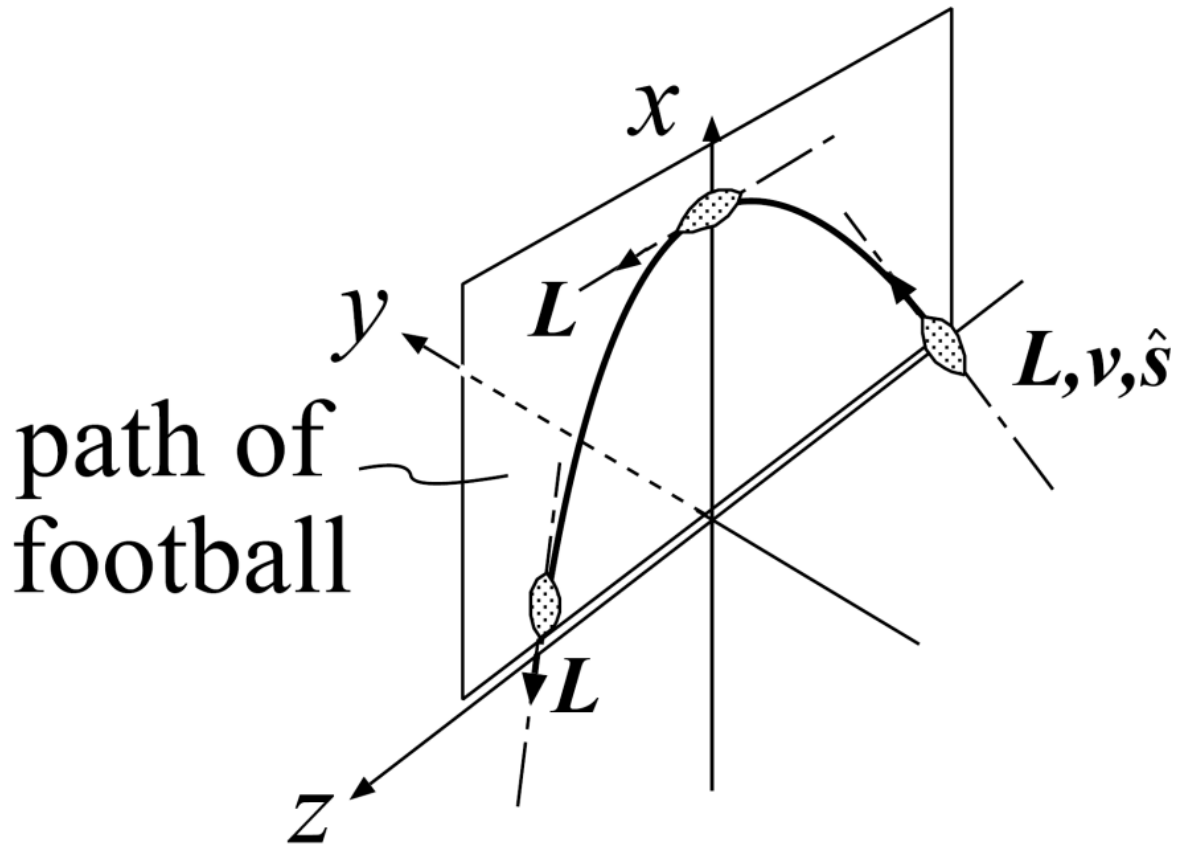


Figure 1. Geometry for the analysis of the flight of an American football, showing the Cartesian coordinate system to be used. A “well-thrown” tight spiral pass is one in which the longitudinal ball axis (corresponding to unit vector \hat{s}), its angular momentum \mathbf{L} , and the velocity \mathbf{v} of the ball’s center of mass (CM) are all co-linear at the point of launch. For a right-handed quarterback, \mathbf{L} points in the same direction as \mathbf{v} .

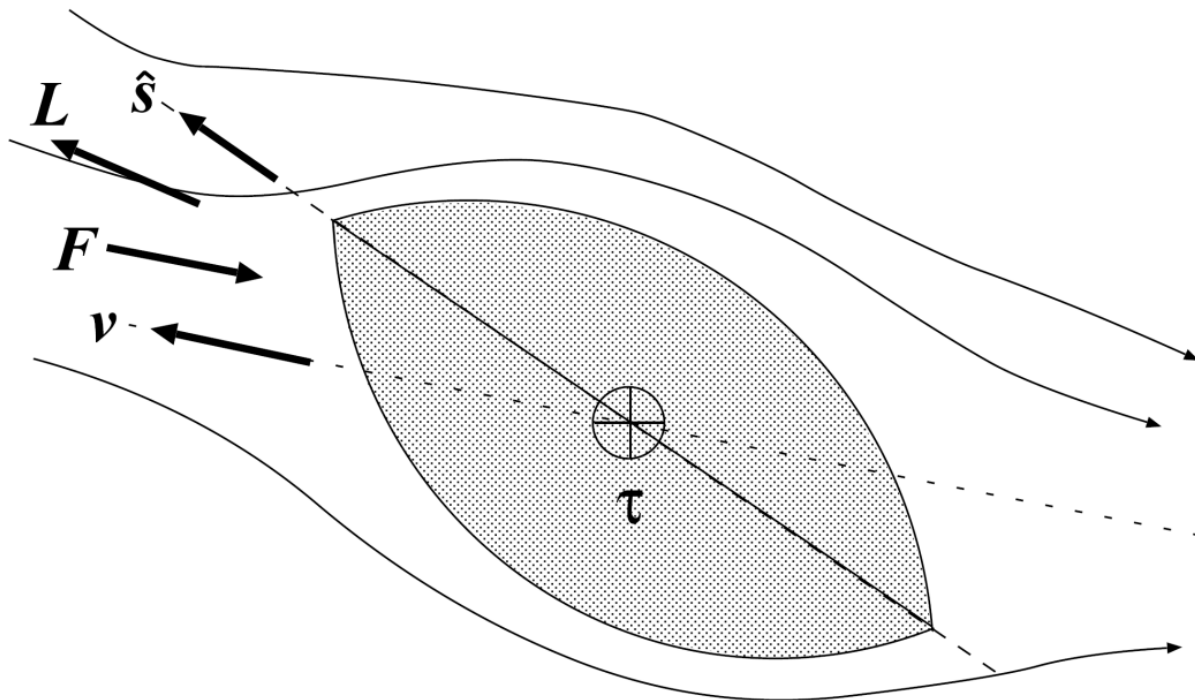


Figure 2. *Airflow past an ascending football with positive pitch. The air drag can be characterized by a single force applied at the “center-of-force” point that leads to an aerodynamic torque $\boldsymbol{\tau}$ about the ball’s center of mass. If \mathbf{v} and the symmetry axis $\hat{\mathbf{s}}$ lie in the plane of the page, then $\boldsymbol{\tau}$ points into the page. Air streamlines are indicated by the curved lines. Since \mathbf{L} and $\hat{\mathbf{s}}$ are not generally co-linear, the ball can wobble with a motion akin to torque-free precession^{1,3}.*

QUANTITY	VALUE	SOURCE
θ ; launch angle	30°	Ref.1
v_0 ; launch speed	27.4 m/s	Ref.1
T ; flight duration	2.80 s	drag-free trajectory
R ; range of flight	66.4 m	drag-free trajectory
I_t ; transverse moment of inertia	$3.21 \times 10^{-3} \text{ kg m}^2$	Ref.1
I_l ; longitudinal moment of inertia	$1.94 \times 10^{-3} \text{ kg m}^2$	Ref.1
τ^* ; torque constant	0.308 N m	Refs.1,5
ω_{spin} ; ball's spin rate	62.8 rad/s	Ref.1
ω_{wob} ; ball's wobble rate	38.0 rad/s	Eq. (5)
ω_{gyr} ; gyroscopic precession rate	2.53 rad/s	Eq. (6)
L ; ball's angular momentum	$1.22 \times 10^{-1} \text{ kg m}^2/\text{s}$	$I_t \omega_{spin}$

Table 1. Parameters for a “long bomb.” See text.

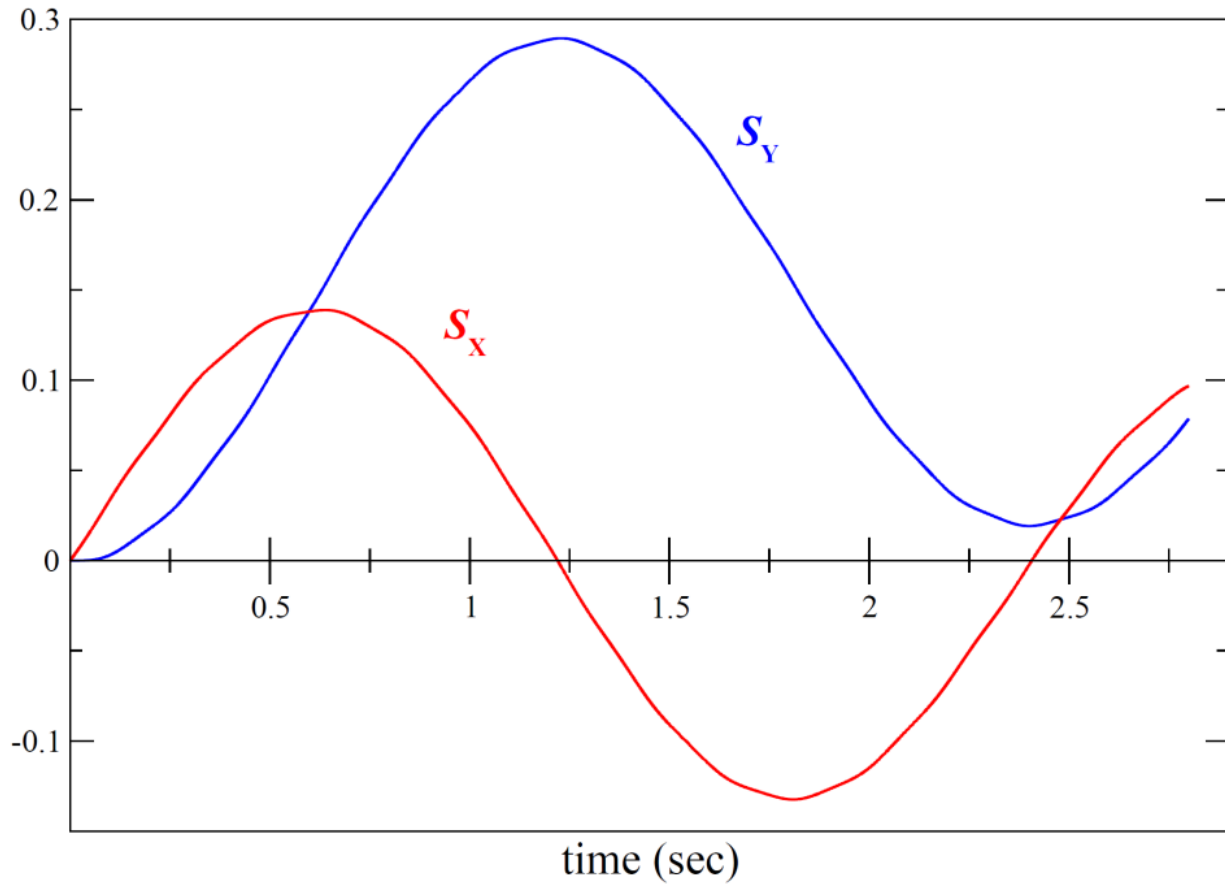


Figure 3. The pitch S_x and yaw, S_y as functions of time, for the 2.8 s of the flight of the “long bomb” pass model described in the text with initial attitude $S_x = 0$ and $S_y = 0$. The values of S_x and S_y are the cosines of the angles between \hat{s} and \hat{X} , and \hat{s} and \hat{Y} , respectively.

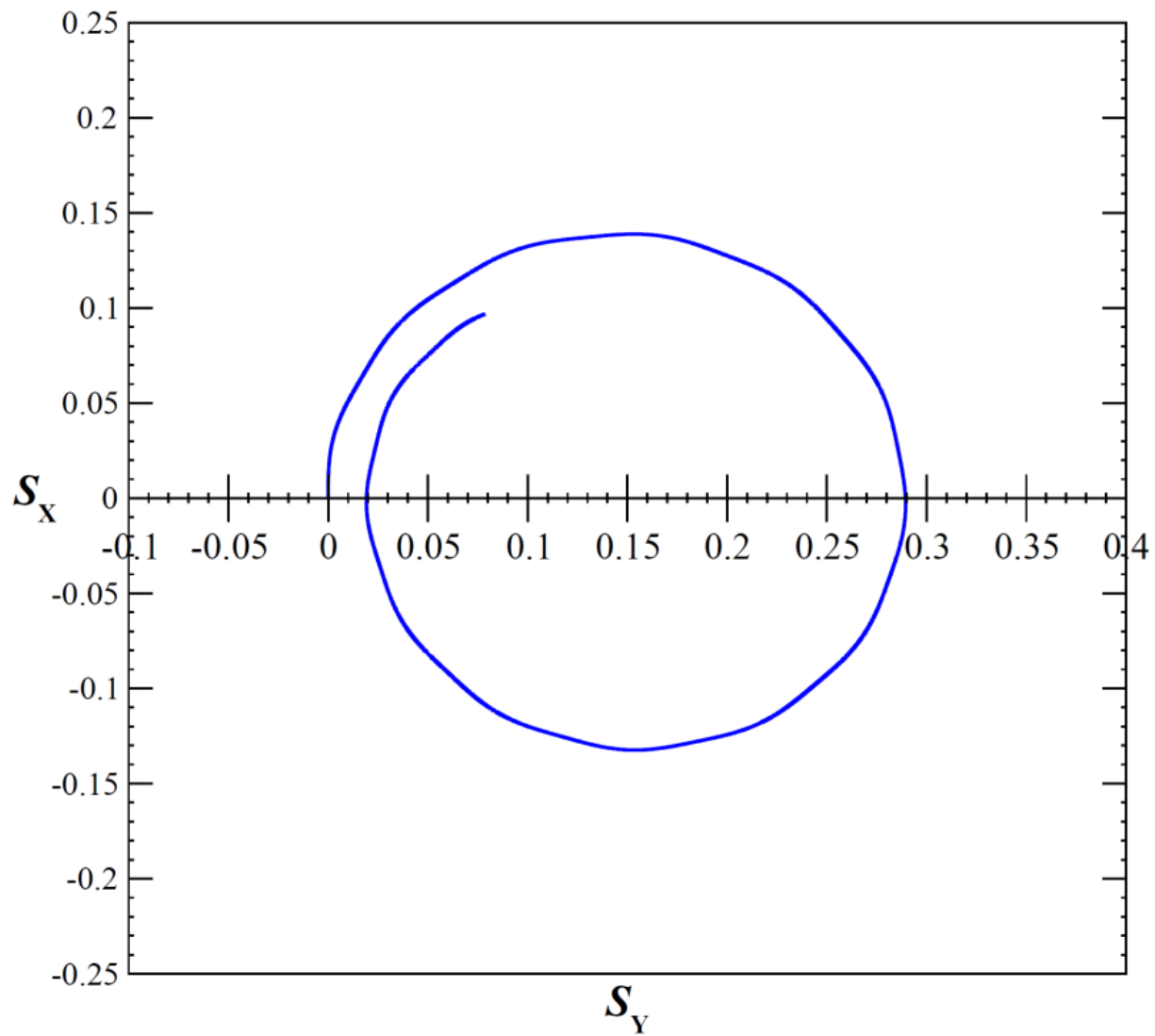


Figure 4. *The path of the tip of the deviation vector \mathbf{S} for the 2.8 s flight of the pass with initial attitude $S_x = 0$ and $S_y = 0$.*

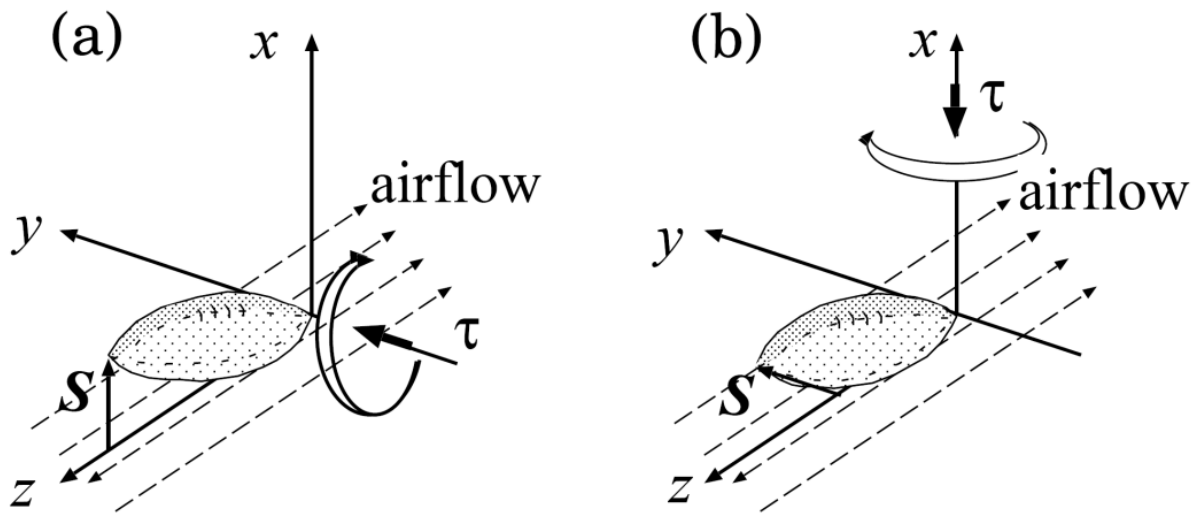


Figure 5. A pictorial representation of the torques for a precessing football moving in the positive z direction with gravity turned off. Shown on the left is the start of the motion with a deviation of $\hat{\mathbf{s}}$ in the positive x direction. The torque due to the airflow is shown as a directed circular arc. This torque in the positive y direction results in the configuration shown on the right, in which $\hat{\mathbf{s}}$ has a deviation in the positive y direction. In this figure the aerodynamic (“yaw”) torque, now in the negative x direction, is again shown as a directed circular arc.

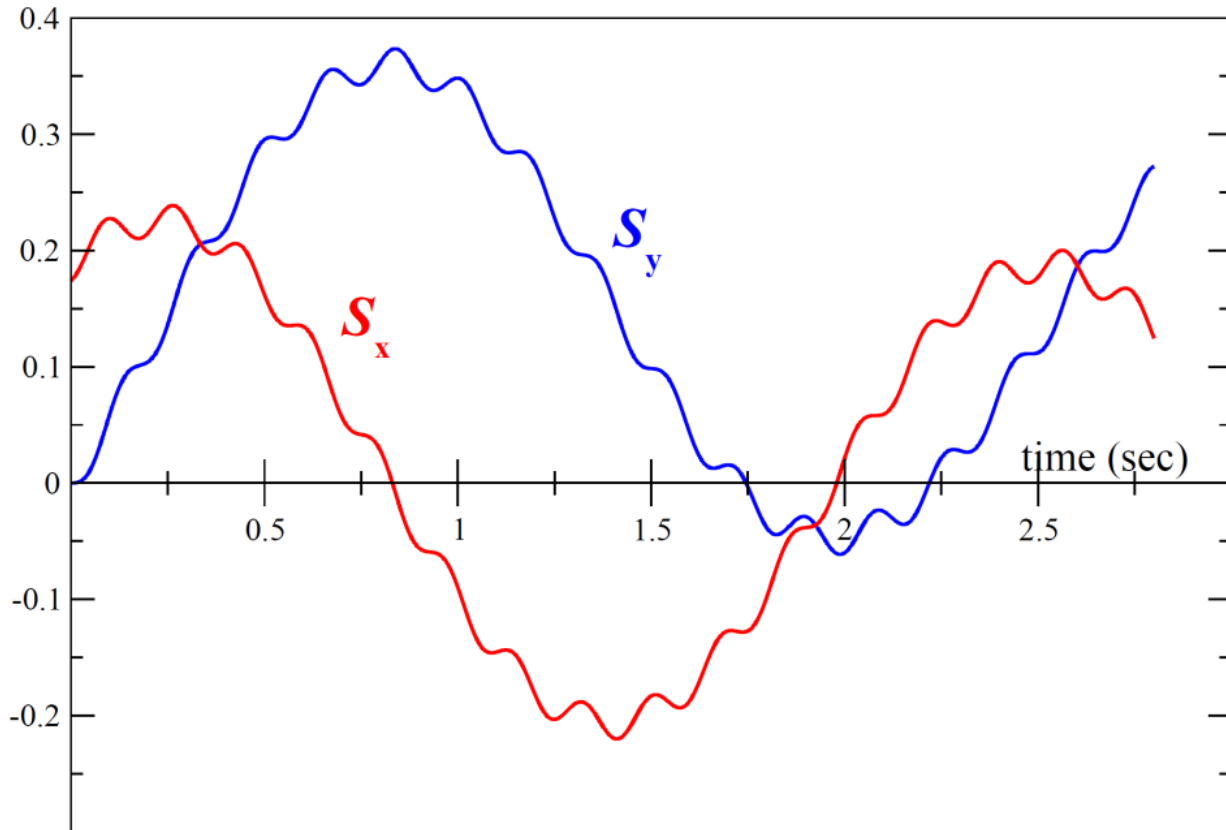


Figure 6. The pitch S_x and the yaw S_y as functions of time, for the 2.8 s of the flight. The values of S_x and S_y are the cosines of the angles between \hat{s} and \hat{X} , and \hat{s} and \hat{Y} , respectively.

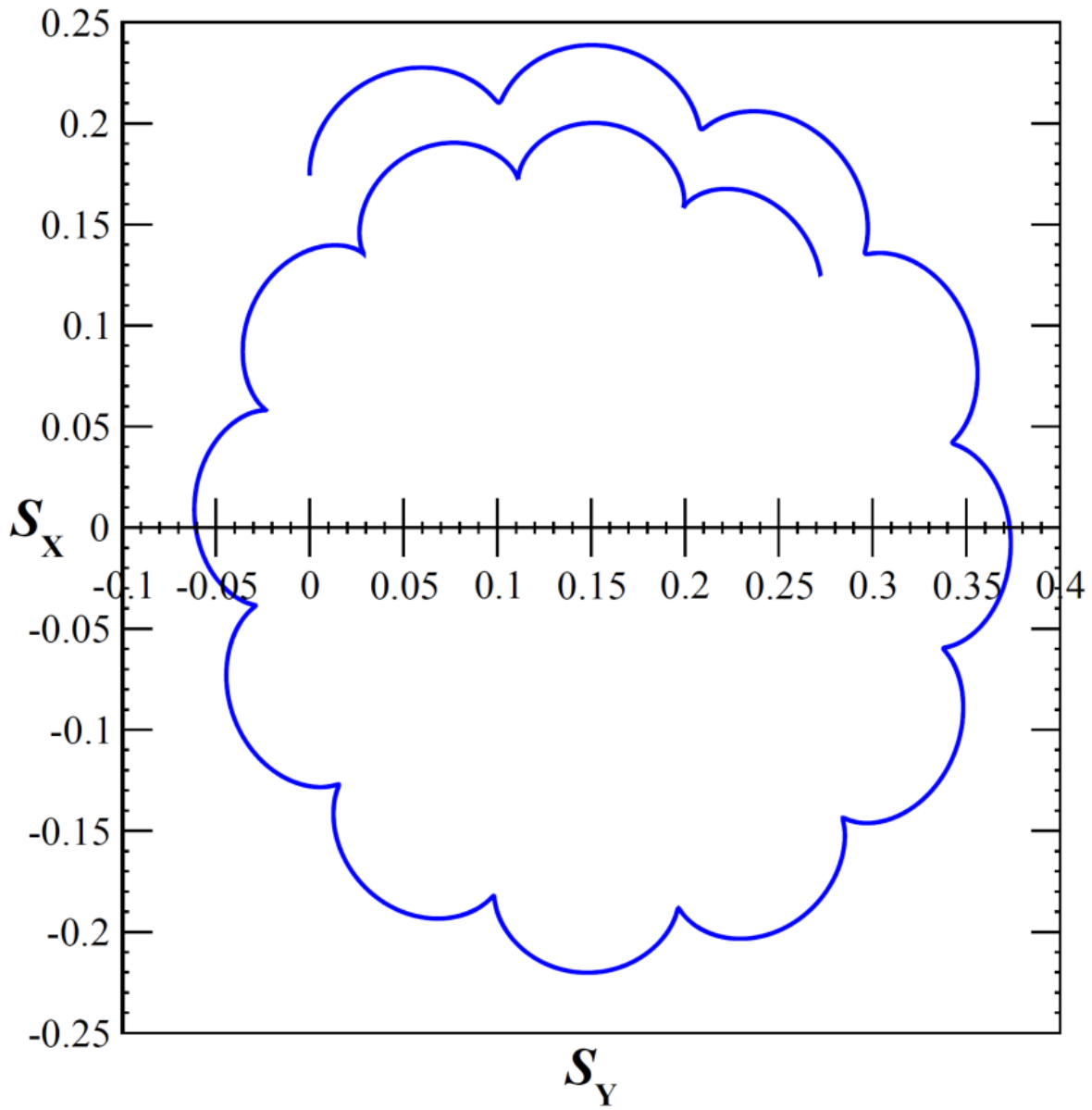


Figure 7. The path of the tip of the deviation vector \mathbf{S} for the 2.8 s of the flight with initial attitude $S_x = 0.175$ and $S_y = 0$.

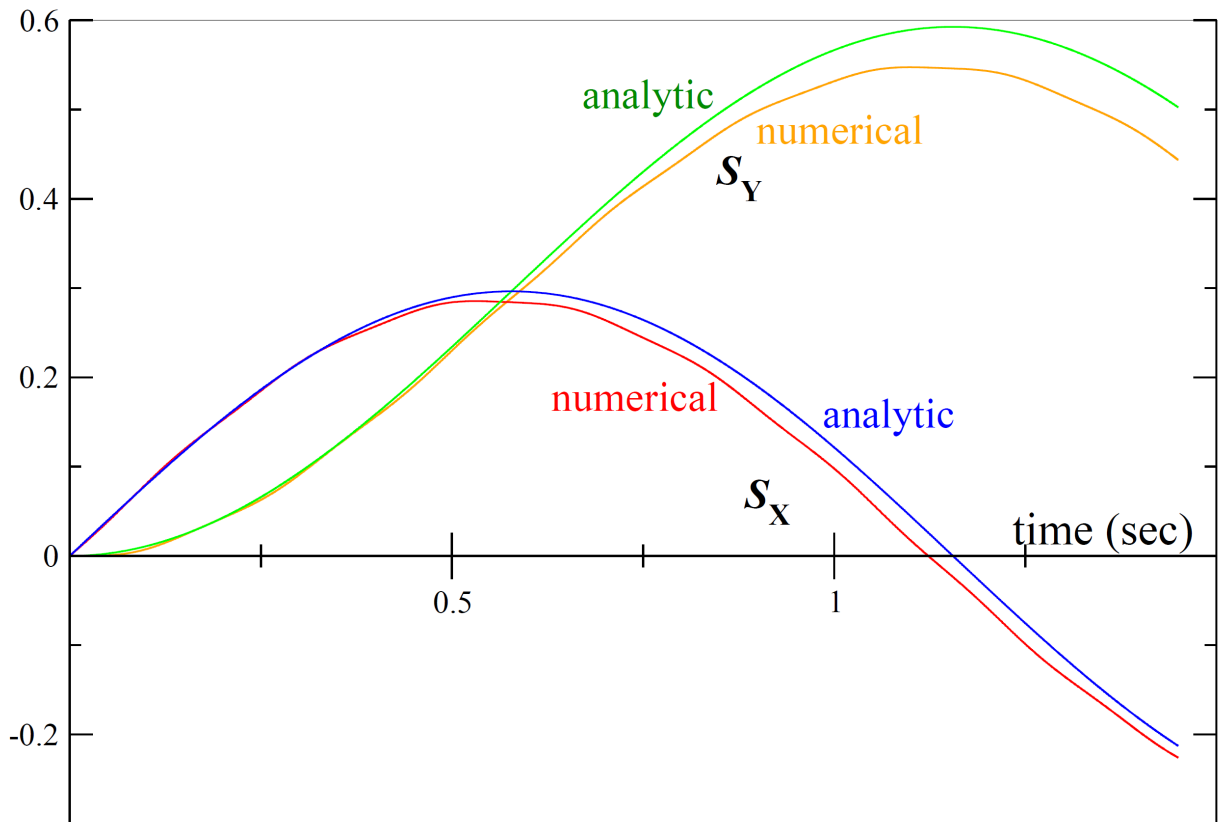


Figure 8. Analytic yaw and pitch for a model with the parameters of the “long bomb” but with the gravity-induced rotation of the velocity replaced by rotation at a constant rate. The comparison is given of numerical results and of a simple analytic model based on the assumption that the symmetry axis remains aligned with the angular momentum, and that the angular momentum magnitude has negligible variation during the motion.